



Changes in monsoon precipitation patterns over Bangladesh and its teleconnections with global climate

Md. Abul Kalam Azad¹ · Abu Reza Md. Towfiqul Islam¹ · Kurratul Ayen¹ · Md. Siddiqur Rahman² · Shamsuddin Shahid³ · Javed Mallick⁴

Received: 29 November 2021 / Accepted: 20 February 2022 / Published online: 9 March 2022
© The Author(s), under exclusive licence to Springer-Verlag GmbH Austria, part of Springer Nature 2022

Abstract

Understanding changes in monsoon precipitation patterns is crucial as it determines the occurrence, intensity, and duration of floods and droughts in Bangladesh. This study investigates changes in monsoon precipitation patterns in different intensities and durations over Bangladesh and their possible teleconnection with large-scale atmospheric oscillations. The changes in different thresholds at 29 stations in Bangladesh were analyzed using the Mann–Kendall (MK) test. Pearson correlation, wavelet coherence (WTC), and multiple wavelet coherence (MWC) methods were also employed to analyze and understand the potential linkage between the large-scale atmospheric circulations and monsoon precipitation indices. The results showed a significant decreasing trend in light and moderate precipitation indices, P10, D10, P20, and D20, while an increasing trend in heavy precipitation indices such as P60, D60, P60plus, and D60plus. The Pearson correlation analysis exhibited a significant correlation between the monsoon precipitation indices and the atmospheric circulation indices. WTC analysis revealed substantial coherence in the time–frequency bands of P10–Nino3.4, D10–Nino3.4, P20–SASMI (South Asian Summer Monsoon Index), P20–EASMI (East Asian Summer Monsoon Index), D20–SASMI, and P60plus–SOI (Southern Oscillation Index) indices. MWC analysis affirmed the correlation and showed the influence of the ERA5 reanalysis parameters, i.e., temperature (T850) and geopotential height at 850 hPa (G850), mean total precipitation rate (MTPR), mean vertically integrated moisture divergence (MVIMD), and summer evaporation (SEV) on the monsoon precipitation indices. The circulation pattern changes, like increasing sea surface temperature, T850, and G850, MTPR, SEV, and decreasing MVIMD, might work as the drivers of monsoon precipitation changes in Bangladesh. The findings can be helpful to address agro-economy losses due to monsoon variability through agricultural planning, flood, landslide and water resources management.

Keywords Monsoon precipitation · Trend analysis · MK test · Ocean-atmospheric circulation · Bangladesh

1 Introduction

The monsoonal system is one of the most crucial elements of the Earth's hydrological cycle and a vital determinant of the functionality of global circulation and environmental systems. It is perhaps the main determinant of precipitation climatology of south and east Asia (Serreze and Barry, 2010). The timing of monsoon arrival and its precipitation intensity and duration determine crop yields, hydroelectric production, forest vegetation, water resources, and ecology in the region (Turner and Annamalai, 2012; Mie Sein et al. 2015; Yeşilırmak and Atatanır, 2016; Zeng et al. 2019; Dubache et al. 2019). Intense and more prolonged precipitation in monsoon may lead to flood, whether the reverse condition may lead to drought. It also plays a crucial role in transferring heat from the tropic to higher latitude areas

✉ Md. Abul Kalam Azad
suborno19@gmail.com

✉ Abu Reza Md. Towfiqul Islam
towfiq_dm@brur.ac.bd

✉ Javed Mallick
jmallick@kku.edu.sa

¹ Department of Disaster Management, Begum Rokeya University, Rangpur 5400, Bangladesh

² Department of Geography, University of Alabama, Tuscaloosa, AL 35487, USA

³ Department of Water & Environmental Engineering, School of Civil Engineering, Universiti Teknologi Malaysia (UTM), 81310 Johor, Malaysia

⁴ Department of Civil Engineering, King Khalid University, Abha 62529, Saudi Arabia

and regulating the Earth's temperature (Loo et al. 2015). The monsoon precipitation patterns showed a significant change in recent years due to climate change (Guilbert et al. 2015; Zhang et al. 2017). Most climate models projected an increase in precipitation extremes under global warming (Zhang et al. 2018). The consequences can be the increasing likelihood of heavy precipitation events and growing drought-hit areas (Ashfaq et al. 2009; IPCC, 2013; Singh et al. 2014; Xu et al. 2020), which can pose an imminent threat to the livelihood of a vast population (Safdar et al. 2019). Besides, extreme precipitation scenarios are estimated to be more frequent in the upcoming years over South Asia under the changing climate (Donat et al. 2016; Islam et al. 2021a). The effect would be much more severe for a densely populated agricultural-based country like Bangladesh, where a slight variability in timing and the amount of monsoon precipitation can severely affect agricultural productivity, food security, and people's livelihood (Matsumoto, 1988).

Bangladesh receives almost 71% of its total annual precipitation during the monsoon (Islam et al. 2019). Some of the heaviest precipitation events in the world occur in Bangladesh during the monsoon (Matsumoto, 1988). This enormous precipitation amount often causes severe floods in the country. The country experienced some of the devastating floods in recent years, which on average caused an economic loss of \$2.2 billion, equivalent to 1.5% of the country's gross domestic product (GDP) (Ozaki, 2016). Flood in 1998 inundated nearly 60% of the land and caused economic damage equivalent to 8% of the country's GDP. Projections of climate models suggest that the global precipitation system will undergo many adjustments, which would profoundly impact extreme weather events like thunderstorms (Azad et al. 2021), droughts, and floods in many Asian countries, including Bangladesh. Therefore, a better understanding of monsoon precipitation changes in Bangladesh and their relation to different ocean-atmospheric oscillation indices and large-scale monsoon circulation patterns is vital for Bangladesh.

Many studies have been conducted for characterization of monsoon precipitation globally (Wang et al. 2012) and regionally, e.g., Asia-Australia (Meehl et al. 2012), South Asia (Turner and Annamalai, 2012), Southeast Asia (Loo et al. 2015), East Asia (Yang et al. 2019), North America (Luong et al. 2017), China (Huang et al. 2019), Eastern China and Pacific region (Ping et al. 2009), Nepal and Himalayas (Bhatt and Nakamura, 2005), Meghalaya Plateau (Fujinami et al. 2017), Indonesia (Moron et al. 2010), Pakistan (Safdar et al. 2019), India (Chaudhary et al. 2018). These published studies covered a wide range of knowledge, including monsoon precipitation concentration index, precipitation concentration degree, precipitation concentration period, monsoon onset shifting, diurnal and interannual

variability of monsoon season, intra-seasonal variability, and raindrop size characteristics. Besides, forecasting and projection on future monsoon precipitation were examined in several studies (Yang et al. 2019; Loo et al. 2015).

Some studies have also been conducted to evaluate the changes in precipitation patterns of Bangladesh (Ahmed et al. 1996; Rahman et al. 1997; Ahasan et al. 2011; Shahid, 2010; Rahman et al. 2017; Khan et al. 2019; Rahman and Islam, 2019; Islam et al. 2020; Fahad et al. 2021). Most of these studies assessed monsoon precipitation changes based on total precipitation received during the monsoon season or focused on the precipitation of the whole year. However, very few studies attempted to evaluate the spatiotemporal changes in monsoon precipitation intensities and durations (Shahid 2011; Montes et al. 2021), which are extremely important to understand the changes in hydrological hazard potential in the country. Besides, the probable synoptic circulation driving the changes in monsoon precipitation patterns is still less understood in Bangladesh (Rafiuddin et al. 2010; Endo et al. 2015; Hassan et al. 2015). The published studies mainly explored precipitation trends and the possible reason behind such trends. For instance, Rafiuddin et al. (2010) analyzed precipitation characteristics in and around Bangladesh and stated that the monsoon systems are large, stationery, or slow-moving. Hassan et al. (2015) studied the trend and spatial distribution of monsoon precipitation using 12 rain-gauge data for the period 1951–2012. Basher et al. (2018) analyzed extreme rainfall indices trends over northeast Bangladesh during 1984–2016 for pre-monsoon and monsoon seasons using rainfall records of only seven stations. Khan et al. (2019) observed the trends in extreme precipitation and temperature indices in Bangladesh during 1981–2010. Montes et al. (2021) evaluated satellite-derived daily precipitation products based on observational data using percentile and threshold-based indices, characterizing their intensity during the monsoon season in Bangladesh. Fahad et al. (2021) explored the effects of surrounding topography and sea surface temperature on summer monsoon precipitation in Bangladesh and the neighboring areas. Nonetheless, these studies mainly focused on average features or a specific aspect of precipitation activities in providing a general picture of changing patterns in Bangladesh's precipitation. As a result, for this region, a comprehensive investigation on the spatiotemporal variations in monsoon precipitation, concentrating on the entire monsoon, is still required.

But, the monsoon precipitation pattern in Bangladesh may be linked to different ocean-atmospheric indices (Wahiduzzaman and Luo, 2020). Recently, various works addressed the relations between the East Asian summer monsoon index (EASMI) and summer monsoon rainfall throughout the South and East Asian areas (Lin et al. 2019; Chen et al. 2021), since EASMI is recognized as one of

the essential aspects of the Asian monsoon (Li and Zeng, 2003; Wu, 2017). Ocean-atmospheric indices like Nino indices are important determinant for summer monsoon precipitation in Indian region (Shukla et al. 2011). Another ocean-atmospheric index, SASMI, has teleconnection with different precipitation indices used by Rahman and Islam (2019). Southern Oscillation Index (SOI) is also crucial in estimating precipitation in Bangladesh (Rana et al. 2007), while Madden–Julian Oscillation (MJO) has intriguing relationship with extreme precipitation in the Indian sub-continent (Anandh and Vissa, 2020). In contrast, vertically integrated moisture divergence is strongly associated with the tropical atmospheric hydrological cycle on a seasonal scale (Xu et al. 2016), while elevated geopotential height with adequate moisture divergence flux can contribute to precipitation variability in Bangladesh (Rahman and Islam, 2019). An increase in sea surface temperature during summer is generally accompanied by increased precipitation over the tropical area (Roxy, 2014). Salahuddin et al. (2006) found significant teleconnection between SST and summer monsoon rainfall in Bangladesh. Besides, other precipitation-related parameters, like temperature and summer evaporation, can also influence monsoon precipitation in different intensities and durations. However, no attempt has been made so far to investigate the joint influence of these synoptic circulation pattern indices and large-scale circulation indices on the changes in monsoon rainfall patterns in Bangladesh. This highlights the need for an in-depth study to fully understand the spatiotemporal changes in monsoon precipitation patterns and the probable synoptic circulation influencing such changes.

Nevertheless, this study is motivated to answer the following question: How do the monsoon precipitation for different thresholds limits spatiotemporally change over Bangladesh? Is there any teleconnection between the monsoon precipitation indices and ocean-atmospheric oscillation indices? Is the synoptic circulation driving the changes in monsoon precipitation in different intensities and durations? Therefore, the objectives are to (1) investigate the spatiotemporal changes in monsoon precipitation indices over Bangladesh, (2) examine the teleconnection between the monsoon precipitation indices and ocean-atmospheric oscillation indices, and (3) investigate the synoptic circulation patterns influencing the changes in monsoon precipitation over Bangladesh. Compared to earlier research, this study has two novel aspects. First, the changes in monsoon precipitation patterns over Bangladesh is studied using indices that were developed based on suitable threshold limits, particularly for monsoon season precipitation in Bangladesh. Second, this is may be the first attempt to assess both the influences of large-scale circulation and synoptic circulation patterns on the spatiotemporal changes in monsoon precipitation in different threshold limits. The findings can help anticipate the

changes in hydrological hazard potential and draw measures to mitigate their effects.

2 Data and method

2.1 Description of the study area

Bangladesh, a country of South Asia, is geographically located between 20 ° 34' to 26 ° 38' North latitude and 88 ° 01' to 92 ° 42' East longitude. This is the biggest deltaic country on the globe, occupying 147,570 km² area (Fig. 1). The three vigorous rivers Padma, Jamuna, and Meghna, and their tributaries encompass 80% of floodplains in Bangladesh, leaving out only the hilly parts in the northeast and southeast. The alluvial soil in the country is vibrant to floods and droughts. Being exposed to differential warming under the great Himalaya Mountain in the North and the Bay of Bengal (BoB) in the south, the circulation of southwest monsoon and the alteration in precipitation systems dominate the climate of the country (Rahman and Islam, 2019). Overall, the climate is portrayed by pelter-bearing breezes, humbly warm temperatures, and high air moisture. However, this narrow flat lowland between Himalaya Mountain and the BoB is very well suited for developing convection, as the moisture conveyed by the monsoon winds from BoB interacts with elevated regions (Ahmed et al. 2017). As an outcome, floods, thunderstorms, and tidal floods are regular incidents in this country. The country receives overwhelming precipitation, aside from certain parts in the west. Extensive rainfall zones in the North, south, southeast, and upper east annually receive rainfall between 2000 and 2500 mm, and the northern and northwestern parts usually receive annual precipitation from 3800 to 5000 mm (Shahid, 2010). The least rainfall, around 1600 mm, is received mm in the central west. The highest amount of precipitation occurs during the monsoon, from June to September. Monsoon moist wind from the BoB transported to the land by weak tropical depressions causes high precipitation during monsoon (Ahmed et al. 2017). Rainfall in June is crucial for Bangladesh as the rainfed Aman rice productivity mostly depends on it (Ghose et al. 2021).

2.2 Data sources and quality controls

Daily precipitation data of monsoon months (June, July, August, and September) for 38 years (1980 to 2017) from 29 meteorological stations were collected from BMD (Bangladesh Meteorological Department), which are scattering over the country (Fig. 1). Geographical and statistical information such as latitude, longitude, elevation, maximum rainfall, standard deviation, and mean precipitation of the meteorological stations is shown in Table 1.

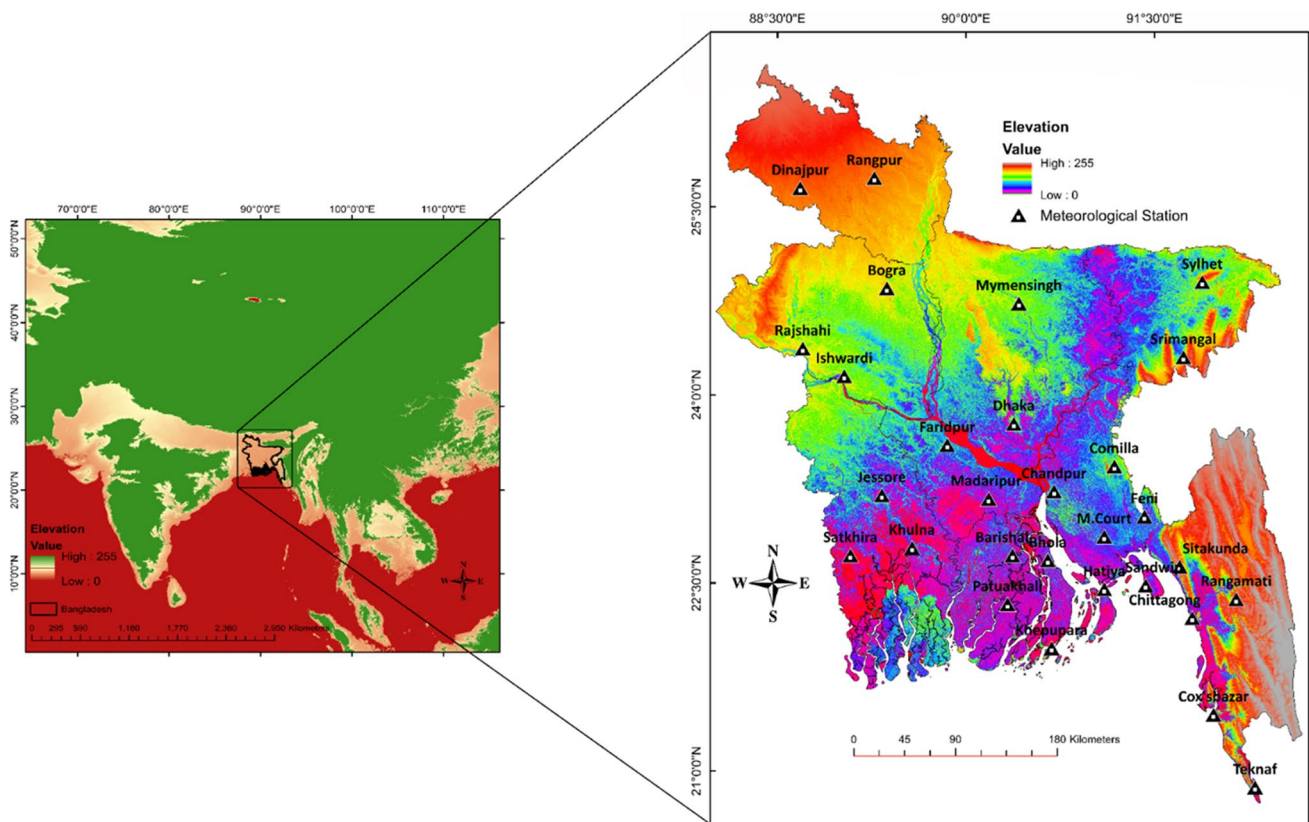


Fig. 1 Geographical location of the study area showing meteorological stations and elevation

Though BMD runs 35 meteorological stations across the country, all of them do not have long-duration data records (BMD, 2018). Twenty-nine stations that have fewer missing values were selected for this study. These sites have missing values below 5% during the study period. The missing values were filled using the daily rainfall records of the adjacent stations. Detailed information about the missing datasets and their filling process is provided in Table S1. For assuring the quality of the data, all records were also validated by the BMD personnel after a data quality check. Albeit, one of the major impediments of trend analysis is the serial correlation in data series. Hence, the auto correlation function (ACF) was used to identify the presence of significant autocorrelation in the data series (Fig. S1). The pre-whitening approach was employed to eliminate the autocorrelation in the specified rainfall time series. Afterwards, the results suggested the absence of serial correlation in time series at most of the stations. Besides, the Standard Normal Homogeneity Test (SNHT) was performed on precipitation series at each station at a significance level ($p < 0.05$) to assure the quality of the data. The test results elicited that the datasets are uniform and homogenous at all stations.

The monthly data of Nino3.4, SOI (Southern Oscillation Index), SASMI (South Asian Summer Monsoon Index), EASMI (East Asian Summer Monsoon Index), and MJO

(Madden–Julian Oscillation index) for the monsoon months, June to September, for the period 1980–2017 were used to assess their influence on monsoon precipitation. The Nino3.4 and SOI data were collected from the NOAA Earth System Research Laboratory (<https://www.esrl.noaa.gov/psd/data/climateindices/>), the SASMI and EASMI dataset were obtained from the NCEP/NCAR monthly analysis dataset (<http://jlp.gcess.cn/dct/page/1>), and the MJO dataset was acquired from National Weather Service of NOAA (https://www.cpc.ncep.noaa.gov/products/precip/CWlink/daily_mjo_index/pentad.shtml).

The European Centre for Medium-Range Weather Forecasts (ECMWF) reanalysis, ERA5, was used to identify the synoptic atmospheric circulations responsible for monsoon precipitation changes in Bangladesh. For this purpose, ERA5 data of sea surface temperature (SST), air temperature (T850), geopotential height at 850 hPa (G850), wind speed, mean vertically integrated moisture divergence (MVIMD), mean total precipitation rate (MTPR), and summer season evaporation (SEV) indices having a spatial resolution of $0.25^\circ \times 0.25^\circ$ were collected for a selected domain of 0 to 50° north and 60 to 120° east, for the period 1980–2017 from the ECMWF website, <https://www.ecmwf.int/en/forecasts/datasets/reanalysis-datasets/era5>. We have used these data using GrADS 2.0.2.oga.2 software where the data were

Table 1 List of stations with latitude, longitude, and elevation; maximum, minimum, and mean monsoon precipitation per year and their standard deviation in Bangladesh

Station name	Latitude	Longitude	Elevation (m)	Maximum (mm)	Minimum (mm)	Mean (mm)	Standard Deviation
Barishal	22.72	90.37	2.1	2128	978	1447.947	279.3569
Bhola	22.68	90.65	4.3	2500	1032	1590.763	319.7671
Bogura	24.85	89.37	17.9	1962	678	1238.921	319.3836
Chandpur	23.23	90.7	4.88	2967	842	1476.868	448.1323
Chattogram	22.22	91.8	5.5	3605	1358	2301.632	578.7649
Coxsbazar	21.45	91.97	7.5	4248	812	2894.368	602.0968
Cumilla	23.43	91.18	2.1	1978	813	1338.368	286.4941
Dhaka	23.77	90.38	8.45	2120	764	1349.711	351.3911
Dinajpur	25.65	88.68	37.8	2737	812	1487.263	376.3255
Faridpur	23.6	89.85	8.1	1760	766	1202.526	269.8835
Feni	23.03	91.42	6.4	3051	503	2118.316	464.6527
Hatiya	22.45	91.1	2.44	3288	29	2386.342	573.3883
Ishwardi	24.15	89.03	12.9	1449	573	1030.842	239.6395
Jashore	23.2	89.33	6.1	1967	675	1187.842	270.4933
Khepupara	21.98	90.68	1.83	2739	1422	2037.105	323.6983
Khulna	22.78	89.57	2.1	2046	720	1299.447	310.4086
M.Court	22.87	91.1	4.87	4010	1512	2295.079	481.2698
Madaripur	23.17	90.18	7	2311	826	1363.132	323.1732
Mymensingh	24.73	90.42	18	2325	947	1518.947	342.6904
Patuakhali	22.33	90.33	1.5	3217	1289	1941.158	380.8873
Rajshahi	24.37	88.7	19.5	1821	507	1052.342	259.9609
Rangamati	22.37	92.15	68.89	2930	1023	1791.158	472.4906
Rangpur	25.73	89.27	32.61	2861	861	1652.895	413.4627
Sandwip	22.48	91.43	2.1	4516	1007	2695.211	676.1439
Satkhira	22.72	89.08	3.96	1733	743	1217.395	241.0604
Sitakunda	22.63	91.7	7.3	3869	359	2323.526	681.5339
Sreemangal	24.3	91.73	21.95	2675	947	1419.026	328.4128
Sylhet	24.9	91.88	33.53	3958	1367	2724.974	559.4929
Teknaf	20.87	92.3	5	4939	1080	3517.789	632.0583

presented as the mean of the selected time series. Time series data of T850, G850, MVIMD, SEV, and MTPR at the observed station's location were extracted and then averaged to derive the country average. These data were used to quantify their association with the precipitation indices through Pearson correlation and multiple wavelet coherence. SST was excluded from analyses because the meteorological stations can not represent any SST value.

2.3 Definition of precipitation index based on threshold limits

Precipitation can be classified in many ways, based on the aim, region, and atmospheric data used, such as thresholds for defining days with precipitation based on fixed values and statistical quantiles (Lupikasza et al. 2011; Rahman and Islam, 2019). Statistical quantiles or percentile-based indices are defined in a way where the categories are not independent

of each other; i.e., heavy precipitation included very heavy precipitation events (Wu et al. 2016). This could make it difficult to quantify the contribution from different category precipitation separately to total precipitation change (Tong et al. 2019). In a subtropical region like Bangladesh, where precipitation days vary significantly from 1 year to another, the same precipitation amount can be distributed into different years for different percentile indices (Rahman and Islam, 2019). It is crucial for flood and drought indication to define thresholds of precipitation amount and number of precipitation days in absolute values. Therefore, we opted for fixed threshold value indices instead of percentiles to define monsoon precipitation patterns. A modified version of the threshold limits used by Khatun et al. (2016) was considered in this study to address precipitation of monsoon months to better understand and evaluate the changes in monsoon precipitation. The precipitation data was divided based on five distinct threshold values to derive ten indices (Table 2), which

Table 2 Description of the monsoon precipitation indices based on the absolute threshold value

Indicator	Descriptive name	Definition	Unit
P10	Light precipitation	Counted as light precipitation when precipitation amount is 4 to 10 mm	mm
D10	Light precipitation days	Precipitation days with 4 to 10 mm precipitation	Days
P20	Moderate precipitation	Counted as moderate precipitation when precipitation amount is 11 to 20 mm	mm
D20	Moderate precipitation days	Precipitation days with 11 to 20 mm precipitation	Days
P35	Moderately heavy precipitation	Counted as moderately heavy precipitation when precipitation amount is 21 to 35 mm	mm
D35	Moderately heavy precipitation days	Precipitation days with 21 to 35 mm precipitation	Days
P60	Heavy precipitation	Counted as moderately heavy precipitation when precipitation amount is 36 to 60 mm	mm
D60	Heavy precipitation days	Precipitation days with 36 to 60 mm precipitation	Days
P60plus	Very heavy precipitation	Counted as very heavy precipitation when precipitation amount is more than 60 mm	mm
D60plus	Very heavy precipitation days	Precipitation days with more than 60 mm precipitation	Days

were light precipitation amount (P10), light precipitation days (D10), moderate precipitation amount (P20), moderate precipitation days (D20), moderately heavy precipitation amount (P35), moderately heavy precipitation days (D35), heavy precipitation amount (P60), heavy precipitation days (D60), very heavy precipitation amount (P60plus), and very heavy precipitation days (D60plus). Among these indices, the light and moderate precipitation indices are almost similar to Khatun et al. (2016), although the moderately heavy, heavy, and very heavy precipitation indices have some modification. Khatun et al. (2016) used the rainfall range of 23–43 mm, 44–88 mm, and above 89 mm to describe moderately heavy, heavy, and very heavy precipitation, respectively. The difference is because of the use of different time scales. Khatun et al. (2016) used the indices to describe the precipitation of the entire year, whereas the present study used only the monsoon season. Besides, most of the years, some sites do not receive heavy precipitation (> 88 mm) in the monsoon season. Therefore, the threshold limits were rearranged to get enough data for all precipitation categories. Here, P10, P20, P35, P60, and P60plus represent total precipitation amount, while D10, D20, D35, D60, and D60plus represent the number of days with respective precipitation limits. Light and moderate precipitation constitute most of the precipitation days. Such events occur throughout the monsoon and maintain soil moisture. Decreases in light and moderate precipitation indices can be indicators for more dry or low rainfall days, while increases in moderately heavy precipitation indices can be indicators for a favorable condition for crop cultivation and better production. The increase in heavy and very heavy precipitation indices indicates a possible increase in floods.

2.4 Wavelet analysis

To evaluate the teleconnection between the monsoon precipitation indices and the large-scale ocean-atmospheric indices, wavelet transform coherence (WTC) and multiple

wavelet coherence (MWC) were employed. WTC and MWC are widely utilized in the environment, geophysics, weather, identifying climatic relationships, etc. (Wang et al. 2019; Lee and Kim, 2019; Islam et al. 2021b; Ng and Chan, 2012; Jerin et al. 2021). Wavelet analysis provides several advantages and flexibilities from a time–frequency point of view. It is very efficient in apprehending nonlinear relationships and identifying significant periods and their changes. The wavelet analysis is also employable to a non-stationary time series. Another advantage is its adaptability to different types of wavelet functions depending upon the nature of data, allowing more efficient and accurate tracking of the co-movements (Rahman et al. 2021). It can also specify the strength and direction of the association, and the difference between short, medium, or long-term relationships (Grinsted et al. 2004).

2.4.1 Wavelet transform coherence

WTC can be used to capture the irregular correlations between two events that are often impossible to get through linear correlation analyses (Islam et al. 2021b). WTC quantifies the covariance magnitude between two time series, varies from 0 to 1 ($0 \leq R^2 \leq 1$). Number 1 refers to perfect coherence, whereas 0 refers to no coherence at all. This range is defined as the cross-spectrum normalized square by the smoothed individual power spectrum. The greater the coherence, the more the symphony between two-time series. The coherence can be defined simply by the following equation:

$$R^2(m, n) = \frac{|S(s^{-1}W_{xy}(s))|^2}{S(s^{-1}|W_x(s)|^2) \cdot S(s^{-1}|W_y(s)|^2)} \quad (1)$$

where x and y are two time series with their respective wavelet transforms $W_x(s)$ and $W_y(s)$. s indicates the smoothing

over both time and scale. The Monte Carlo simulation method was employed here to get the result.

Wavelet transform coherence method additionally reveals the phase shift across the time dimension by specifying an angle in an interval (Lee and Kim, 2019). The angle can be stated as a phase difference; this reveals that the shared cycles between the two data sets are negatively or positively associated. This also displays which data series is ahead in terms of the relationship between the data series at specific frequency levels. Right-pointing arrows depict that the two signals are in-phase, while left-pointing arrows indicate an anti-phase signal; down-pointing arrows indicate that the precipitation indices are ahead of the ocean-atmospheric index, while up-pointing arrows indicate that the indices lag behind the ocean-atmospheric index.

2.4.2 Multiple Wavelet Coherence

MWC can examine the temporal variability influenced by multiple factors in different time scales. Therefore, it provides a better understanding of the underlying processes responsible for the change in the examined variable (Rahman et al. 2021). In MWC, the influence of two time series' (x_1 and x_2) on the response series (y) can be estimated using the following equation:

$$RM^2(y, x_1, x_2) = \frac{R^2(y, x_1) + R^2(y, x_2) - 2Re[R(y, x_1) \cdot R(y, x_2) * R(x_2, x_1) *]}{1 - R^2(x_2, x_1)} \quad (2)$$

The Sen's slope estimator, introduced by Sen (1968), was used to quantify the slope of a trend in monsoon precipitation indices. The Mann–Kendall (MK) test was used to detect the significance of the trends (Kendall, 1975; Mann, 1945). Details of the MK test and Sen's slope estimator can be found elsewhere in the literature (Li et al. 2018; Rahman and Islam, 2019). The sequential version of the MK test was also applied to detect an abrupt change in the monsoon precipitation time series. Details of this method can be found in Praveen et al. (2020) and Islam et al. (2021a). The bivariate Pearson correlation coefficient was also employed to demonstrate the correlation between the monsoon precipitation indices with large-scale ocean-atmospheric indices and ERA5 variables.

3 Results

3.1 Changes in monsoon precipitation indices

The areal average annual series of monsoon precipitation indices (Fig. 2) showed that P10 (Fig. 2a), D10 (Fig. 2b), P20 (Fig. 2c), and D20 (Fig. 2d) indices were decreasing at a rate of 0.254, 0.031, 0.281, and 0.021 per year, respectively. The decreases were significant at $p < 0.05$. It indicates

that light and moderate precipitation amounts and days are decreasing remarkably, which might increase the frequency of short-term droughts. No significant change was detected for P35 (Fig. 2e) and D35 (Fig. 2f) during 1980–2017. On the contrary, P60 (Fig. 2g), D60 (Fig. 2h), P60plus (Fig. 2i), and D60plus (Fig. 2j) were found to increase at a rate of 0.432, 0.008, 1.136, and 0.018 per year, respectively. Increases in heavy and very heavy precipitation amounts and days imply an increased risk of monsoon floods.

3.2 Spatiotemporal changes in the monsoon precipitation indices

The results of the Sen's slope and MK test for each station were shown in a spatial distribution map (Fig. 3) generated through ArcGIS 10.6.1. The Sen's slope value was shown using Histogram-equalize technique, while the MK test results were represented through multi-color triangle. The MK test statistics for the indices vary between -2.6034 and 2.905 and the Sen's slope between -12.333 and 20.833 . The Sen's slope value (Fig. 3a) for P10 was in the range of -1.125 to 0.8 . It showed a decreasing trend at 59% of the stations. The higher decreases were noticed at 10% of the stations, located in the north-central and southern parts of Bangladesh. The Sen's slope of D10 (-0.147 to 0.068) showed a similar trend pattern (Fig. 3b) like P10. The D10 showed a decreasing trend at 55% of the stations, of which significant decreases were noticed in the southern region. It showed increasing trends at a few stations in the North and eastern parts of the country. The rate of change in P20 was between -3.057 and 0.999 (Fig. 3c), where declining trends were noticed at 55% stations distributed randomly and increasing trends at 28% of the stations, mostly located in the south. The changes in D20 were in the range of -0.166 to 0.095 . It decreased at 52% of the stations distributed randomly over the country while increasing at 28%, predominantly in the south (Fig. 3d). P35 showed a change in the range of -2.992 to 3.466 , while D35 showed a change between -0.107 and 0.140 . The P35 (Fig. 3e) and D35 (Fig. 3f) decreased at 55% and 48% of the stations, respectively, and increased at some stations in the south. In contrast, the P60, D60, P60plus, and D60plus showed changes in the range of -5.393 to 5.107 , -0.083 to 0.105 , -12.333 to 20.833 , and -0.090 to 0.149 , respectively. The P60 (Fig. 3g) and D60 (Fig. 3h) increased at 41% of the stations, mostly located in the southern region, while they showed decreasing trend at 31 to 38% of the stations located in the central and western regions. The P60plus and D60plus showed an increasing trend in the south and decreasing trends in the central and southern regions (Fig. 3i–j). Overall, the results revealed large spatial variability in the trends of different monsoon precipitation indices.

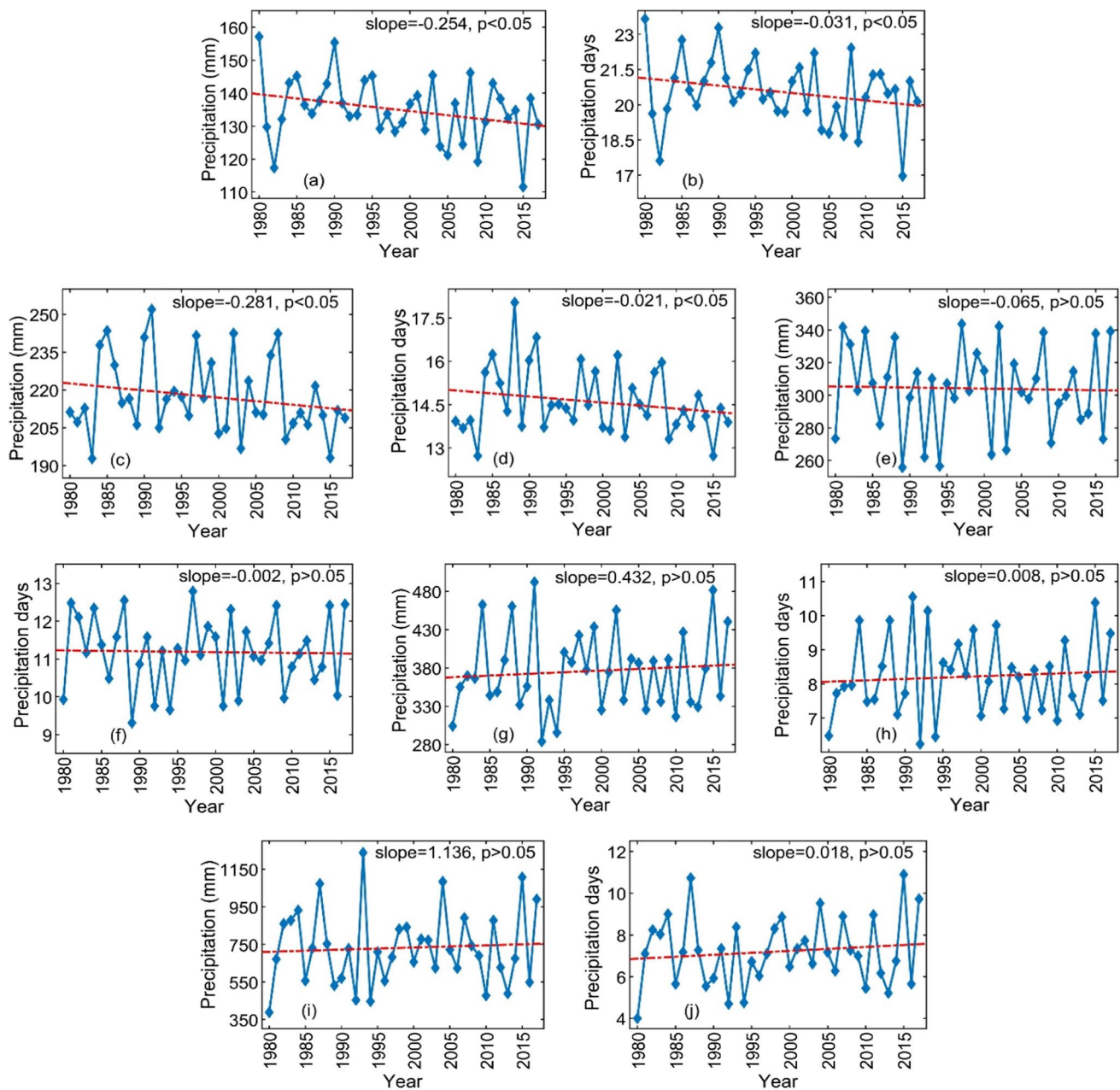


Fig. 2 Linear regression trends for 10 precipitation indices: **a** P10, **b** D10, **c** P20, **d** D20, **e** P35, **f** D35, **g** P60, **h** D60, **i** P60plus, and **j** D60plus in Bangladesh during 1980–2017 (the cyan line is the annual time series of the designated index; the dashed red line is the linear trend line)

3.3 Teleconnection between the monsoon precipitation indices and ocean-atmospheric circulation

3.3.1 Correlation analysis

Five ocean-atmospheric circulation indices (Nino3.4, SOI, SASMI, EASMI, and MJO) and five ERA5 reanalysis indices (T850, G850, MVIMD, MTPR, and SEV) were chosen to assess their influence on monsoon precipitation indices

in Bangladesh. The monsoon months of Bangladesh, such as June, July, August, September, were considered to investigate the teleconnection of rainfall indices with circulation indices. Pearson correlations between the country averages of the monsoon precipitation indices with the large-scale ocean-atmospheric circulation indices and the country averages of the ERA5 reanalysis indices during 1980–2017 are shown in Fig. 4. The correlation analysis revealed that the large-scale atmospheric circulation and ERA5 reanalysis indices were significantly associated with the monsoon

precipitation indices. P10 and D10 showed a significant inverse association with Nino3.4, MJO, and T850. P20 showed a positive correlation with SASMI, EASMI, and SEV but a negative correlation with G850 and MVIMD, while D20 showed a positive correlation with SASMI and a negative correlation with MVIMD. The rest of the monsoon precipitation indices (P35, D35, P60, D60, P60plus, and D60plus) showed no significant association with any circulation indices. However, P60plus showed a high negative correlation with SOI. Therefore, its relation with circulation indices was further investigated along with P10, D10, P20, and D20 using the Wavelet coherence analysis. The indices showed insignificant correlation was not considered for WTC analysis to reduce noise. However, the influence of ERA5 reanalysis variables on the relationship of monsoon precipitation indices with the large-scale atmospheric circulation indices was analyzed using MWC.

3.3.2 Wavelet transform coherence analysis

The wavelet transform coherence between the country averages of monsoon precipitation indices and circulation indices is shown in Fig. 5. P10 and Nino3.4 (Fig. 5a) showed a large coherence during the study period with a cycle of 4.5 to 7.5 years. Another coherence band was noticed from the middle to the end of the study period. The P10 series was ahead of the Nino3.4 series in both cases. A small red island was observed between P10 and MJO (Fig. 5b), having an out-of-phase relationship within the cone of influence during 2002–2007 with a cycle of 2–3 years. WTC between D10 and Nino3.4 (Fig. 5c) also showed two high coherence bands: the first one had an oscillation period of 4.5–7.5 years during 1980–2002, occupying both the inner and outer side of the cone of influence, where the D10 series was leading the Nino3.4 series by 90°; the second one, mostly remained outside the cone of influence, lasts until the end of the time series, where the D10 series was ahead of the Nino3.4 series. For D10 and MJO, only a short out-of-phase coherence was observed during 2003–2005 within the significant area (Fig. 5d).

P20 and SASMI (Fig. 5e) showed significant in-phase coherence during 1986–1997, with an oscillation of 1–5 years. WTC between P20 and EASMI (Fig. 5f) showed three coherence bands within the area of significance. The first one was approximately in-phase during 1990–1995 with an oscillation period of 3.5 to 4.5. Then, a high in-phase coherence in the middle of the time series. The last one shows an out-of-phase relationship during 2010–2013 with an oscillation period of 2–3 years. For D20 and SASMI (Fig. 5g), a significant in-phase coherence was observed during 1985–1990 with an oscillation period of 2 years. P60plus and SOI (Fig. 5h) exhibited a coherence band that occupied

both the insignificant and significant areas. It expanded from the beginning of the time series until 1993 in the 4–7 years oscillation period, where P60plus was ahead of SOI. Overall, the results revealed significant coherence of monsoon precipitation indices with circulation indices, except that the coherence between P10 and MJO and D10 and MJO was not much powerful. Therefore, these two combinations were excluded from multiple wavelet coherence analyses.

3.3.3 Multiple wavelet coherence analysis

MWC is employed to reveal how the linear combination of large-scale atmospheric circulation and ERA5 reanalysis series related to dependent precipitation indices series (Fig. 6). For example, Nino3.4 and T850 were the independent series, and P10 was the dependent series in Fig. 6a.

Figure 6a and b exhibit a large coherence region within the cone of influence, denoting a higher linear relationship of P10 and D10 with the Nino3.4-T850 combination. In both cases, a 3–7.5-year coherence cycle was observed for the whole period and an 8.5–10-year cycle during 1996–2018. MWC between P20 and SASMI-G850 combination revealed a large coherence band, mostly inside the significant area, during 1980–1998 with a cycle of 0–6 years (Fig. 6c). The combination of SASMI-MVIMD elicited some significant short- and long-term coherence with P20 (Fig. 6d). A red-colored band with a thick black contour appeared between 1980 and 1996, with a frequency ranging between 0–4 and 4–8. A second coherence band with an oscillation period of 2–6 years was noticed during 2002–2018, although some of it was outside the significant region. Multiple coherence bands appeared for P20 and SASMI-SEV (Fig. 6e) in the shortest and longest periods. The first band was quite similar to the first band of P20 and SASMI-MVIMD combination, while the second band appeared during 1998–2004 in the 0–2 frequency bands.

The relationship between P20 and EASMI was checked by adding the influence of G850 (Fig. 6f), MVIMD (Fig. 6g), and SEV (Fig. 6h) on EASMI. The results elicited a couple of coherence bands during 1980–1995 with cycles of 0–4 and 4–8 years. A hot region was noticed within the 0–4 time–frequency bands for all three indices. For the P20 and EASMI-MVIMD pair, a long coherence band was found at the top of the cone, running throughout the time series with an oscillation period of 9–10 years. A significant red region with black contour is also visible for the P20 and EASMI-SEV series during 2011–2014. Multiple coherence bands were amalgamated around the center in the MWC between P60plus and SOI-MTPR (Fig. 6i) and P60plus and SOI-MVIMD (Fig. 6j). It reaffirmed the linear relationship and high correlation among the indices. Overall, the results indicate higher coherence between

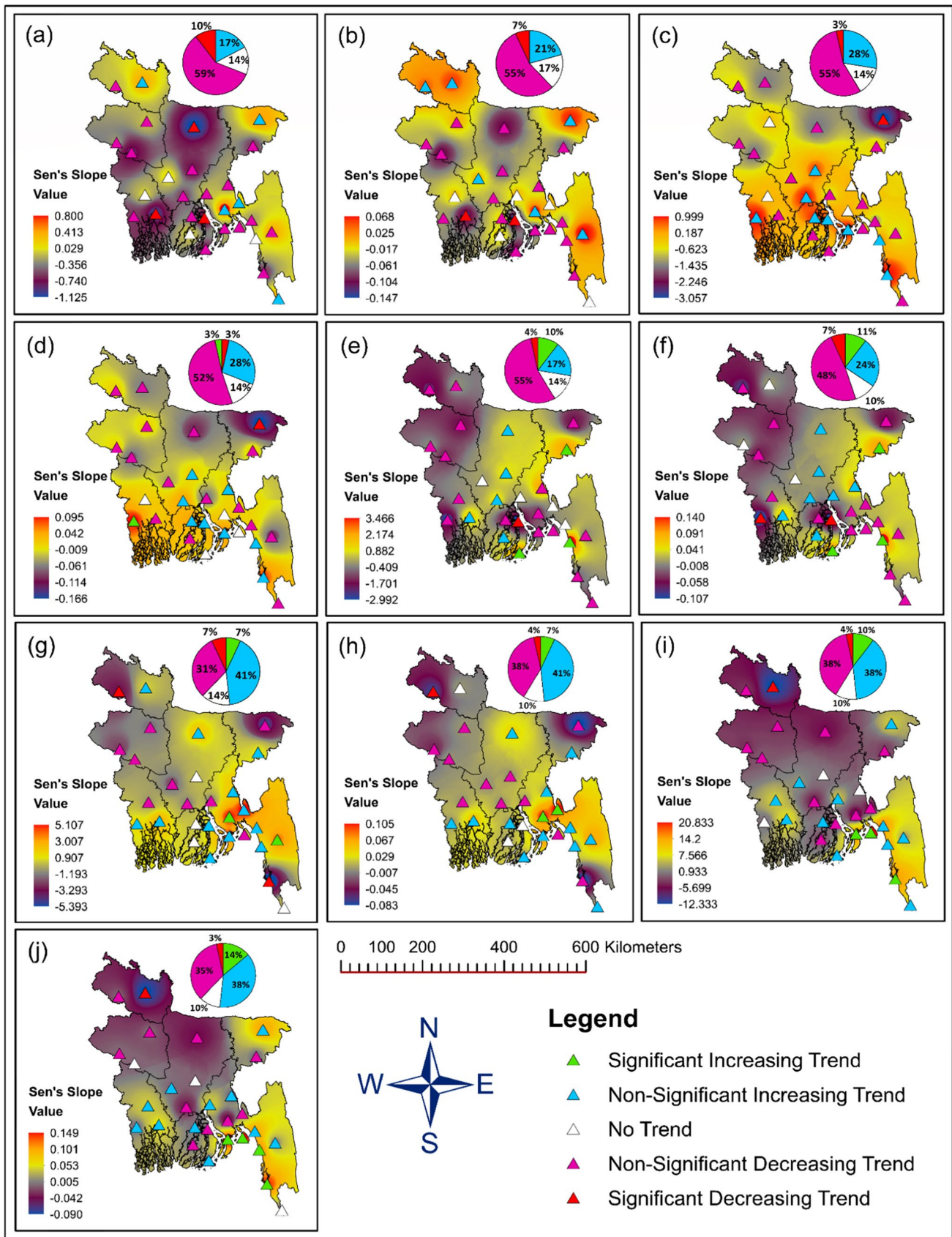


Fig. 3 Spatial distribution of the trends in 10 precipitation indices: **a** P10, **b** D10, **c** P20, **d** D20, **e** P35, **f** D35, **g** P60, **h** D60, **i** P60plus, and **j** D60plus from 1980 to 2017 based on MK Test and Sen's slope analysis

monsoon precipitation and circulation indices when ERA5 reanalysis indices' influence was considered.

4 Discussion

The trend analysis of the monsoon precipitation indices revealed that light and moderate precipitation amounts and days were decreasing, indicating increasing dry or low rainfall days, which can affect Bangladesh's soil moisture. The abrupt shifting of these indices was also noticed, which might be associated with the rapid warming of the sea surface in the Indian Ocean (Fig. 7a), resulting in decreasing precipitation. The land–sea temperature difference (Fig. 7a and b) caused by such warming results in declining precipitation amounts and days over some Southeast Asia regions (Roxy et al. 2015). Moderately heavy precipitation amounts and days showed stationary behavior in this study. They did not exhibit any potential turning point in the time series either. The heavy precipitation amount and days were increasing; among them, the heavy precipitation day index has abrupt shifting in its time series, which might impact flood occurrence in the monsoon season. Shahid (2010) stated that an increase in SST of the Bay of Bengal might cause increased heavy precipitation in Bangladesh, which contradicts our finding as no significant change in SST over the BoB was noticed. Instead, a substantial increase in SST over the Indian Ocean was observed (Fig. 7a). The higher temperature evaporates more water in the Indian Ocean, which is then conveyed by the monsoon wind as moisture and brings downpour. The results obtained in this study aligned with Wu et al. (2016), where they reported similar kinds of precipitation changes in China. Joshi and Rai (2015) identified that the heavy precipitation is decreasing in northeast India during positive Atlantic multi-decadal oscillation (AMO) and negative Inter-decadal Pacific Oscillation (IPO), which also contradicts our findings. In the present study, most precipitation indices showed an increasing trend in the southeastern regions and a decreasing trend in the northeastern region. Rahman et al. (1997) found a changing precipitation pattern at the stations located in the southeast hilly area of Bangladesh. This spatial variation might occur due to an abrupt change in precipitation during 2001 (Fig. S2), which might be caused by the shifting of the synoptic circulation indices (ERA5 reanalysis indices) (Fig. 7) or the weakening of the worldwide monsoon circulation (Chase et al. 2003; Pant, 2003). The difference in ECMWF ERA5 reanalysis datasets for the earlier period (1980–2001) and

the later period (2002–2017) was analyzed to examine the influences of synoptic circulation indices on these increases.

Figure 7b elicits an increase in temperature by 0.2° Kelvin at 850 hPa all over Bangladesh during the monsoon season for the period 2002–2017, which might affect the change in monsoon precipitation. Figure 7c depicts a more remarkable change of geopotential height at 850 hPa during the monsoon season in the northwestern part of Bangladesh and a comparatively lesser change in the country's remaining regions. A significantly greater change in geopotential height was noticed near the Himalayan Mountain ranges, which supports anticyclone formation. The wind circulation brings moisture from the anticyclonic zone to the elevated Shillong plateau and Assam and then enters Bangladesh from the northeastern part and passes through to India's West Bengal. These wet air circulations create a favorable atmosphere for precipitation formation. Figure 7d delineates small changes in mean vertically integrated moisture divergence (MVIMD) in the northern and south-central parts, while no change in other parts of the country might be the reason for spatial variation of precipitation patterns in Bangladesh. Besides, MVIMD decreases significantly near the country's northern boundary causes precipitation intensification and floods in the north region. The total precipitation rate remained stable for most of Bangladesh's territory, but it increased in the northern part (Fig. 7e). Bangladesh's surroundings showed anomalies in the total precipitation rate, which might be a reason for changing precipitation patterns within the country. Apart from these, the variation in land cover and land use may indirectly affect the natural climate system (John et al. 2009). More evaporation from the sea near the BoB coast during the summer (Fig. 7f) season may be a probable cause for increasing heavy or very heavy precipitation in the monsoon season. The higher evaporation makes more moisture available to form a denser cloud and these thicker clouds formed during the summer season carried by wind circulation, which often condensed during the monsoon season and caused increasing heavy precipitation. Besides, the spatial heterogeneity of the heavy precipitation indices can be affected by topography, which is considered a vital factor (Huang et al. 2019).

The influences of the synoptic circulation pattern indices on the monsoon precipitation indices can also be seen in the Pearson correlation and wavelet analysis. The Pearson correlation analysis (Fig. 4) revealed that all the precipitation indices are correlated with most ERA5 reanalysis indices. Besides, WTC (Fig. 5) and MWC (Fig. 6) showed coherence between P10 and Nino3.4, which became stronger under the influence of T850. Likewise, the coherence between D10 and Nino3.4 improved, considering the effect of T850. Similar improvement was also noticed between P20 and SASMI and P20 and EASMI, considering the effects of the ERA5



Fig. 4 Pearson’s correlation coefficient between the 10 thresholds-based monsoon precipitation indices with ocean-atmospheric circulation and ERA5 reanalysis indices in Bangladesh during 1980–2017

(*significant at the $p < 0.05$ level; **significant at the $p < 0.01$ level). The red colored box involves the ocean-atmospheric circulation indices, while the outside of the box contains ERA5 reanalysis indices

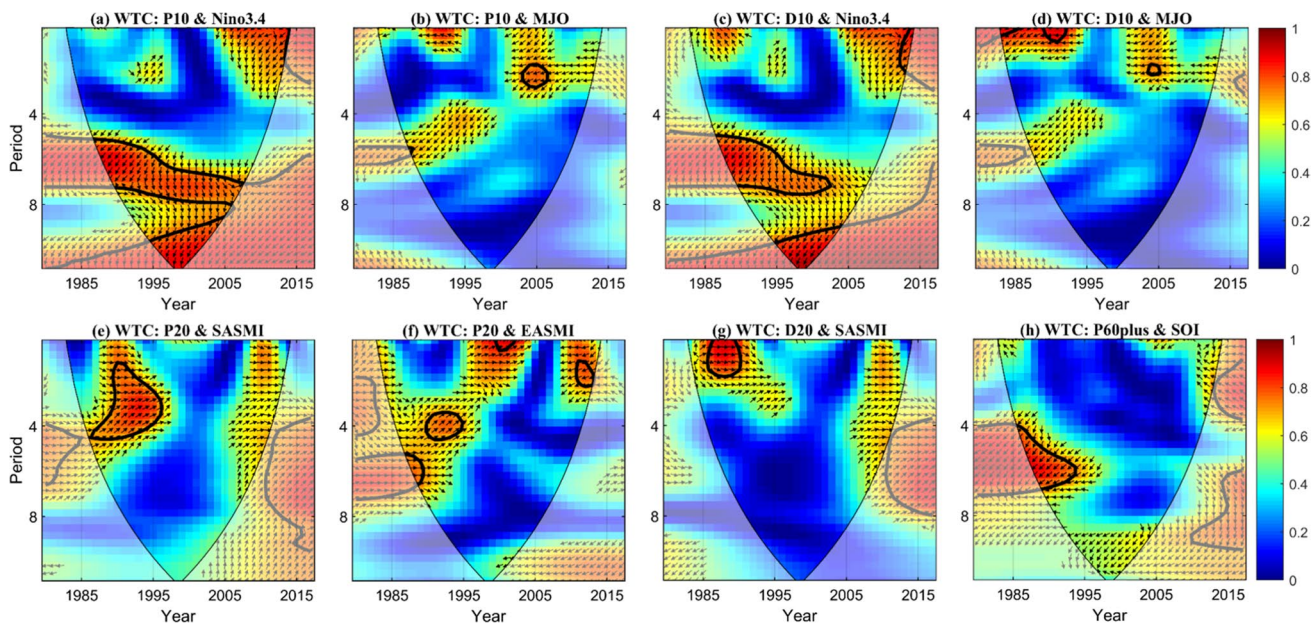


Fig. 5 Wavelet coherence between P10 and Nino3.4 (a), P10 and MJO (b), D10 and Nino3.4 (c), D10 and MJO (d), P20 and SASMI (e), P20 and EASMI (f), D20 and SASMI (g), and P60plus and SOI

(h). The thick black contour is the 95% confidence level, whereas the lighter shade shows the cone of influence

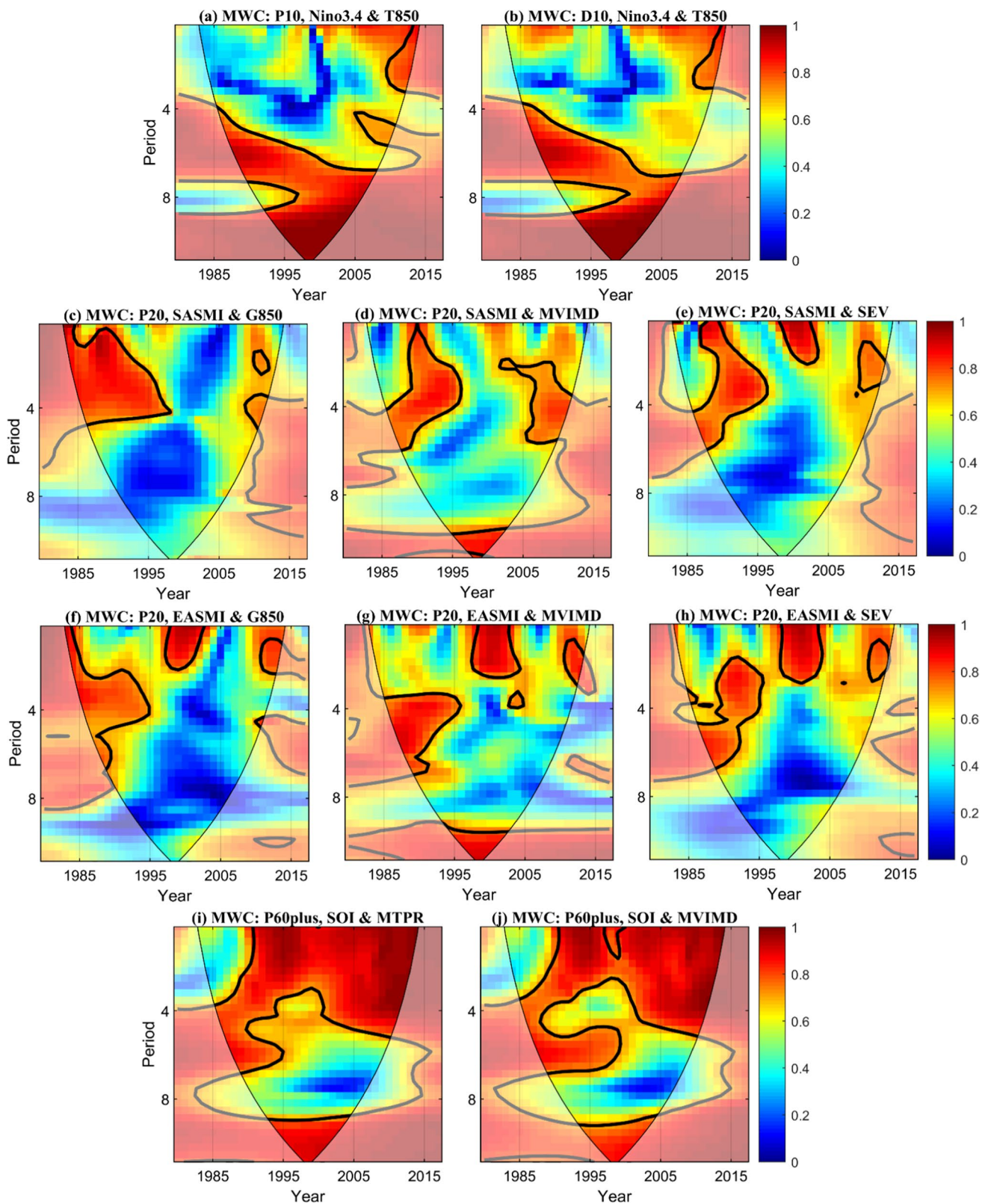


Fig. 6 MWC between P10, Nino3.4, and T850 (a); D10, Nino3.4, and T850 (b); P20, SASMI, and G850 (c); P20, SASMI, and MVIMD (d); P20, SASMI, and SEV (e); P20, EASMI, and G850 (f); P20, EASMI, and MVIMD (g); P20, EASMI, and SEV (h); P60plus, SOI,

and MTPR (i); and P60plus, SOI, and MVIMD (j). The thick black contour is the 95% confidence level, whereas the lighter shade shows the cone of influence

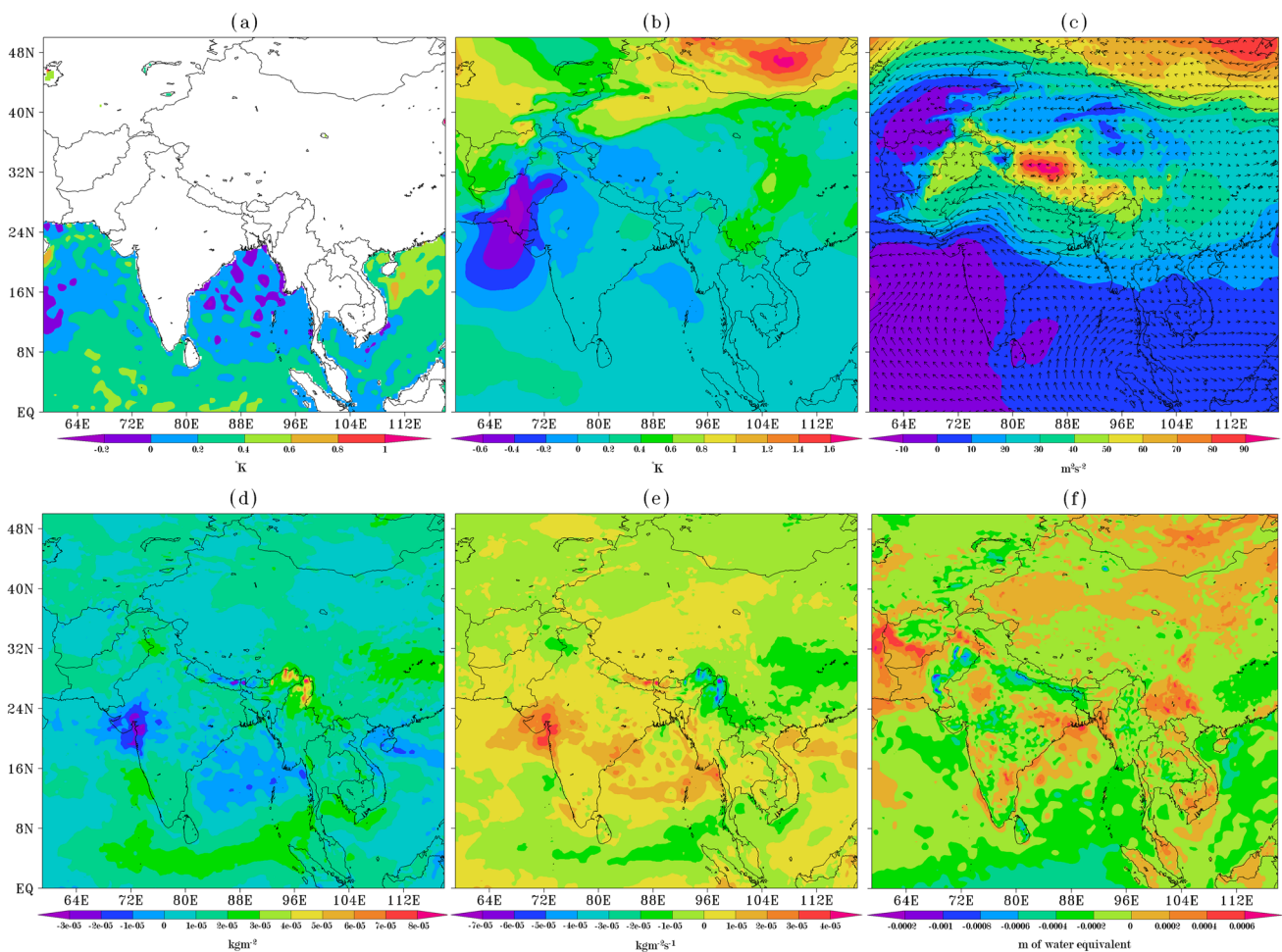


Fig. 7 Spatial differences in the field of sea surface temperature (a), temperature at 850 hPa (b), geopotential height at 850 hPa with wind direction (c), mean Vertically Integrated Moisture Divergence (d),

Total Precipitation Rate (e) and Summer Evaporation (f) at 850 hPa between 2002–2017 and 1980–2001

reanalysis indices like G850, MVIMD, and SEV, and the coherence between P60plus and SOI, considering the influence of MTPR and MVIMD. The results indicate a significant influence of synoptic circulation indices on most monsoon precipitation indices. Apart from this, precipitation is related to altitude in space (Liu et al. 2013) and time (Zhang et al. 2014) at a regional scale. Bangladesh's monsoon comes from the Bay of Bengal and passes through the plain to the North and northeast before being turned to the west and northwest by the Himalayas' foothills (Shahid, 2010). Rahman et al. (1997) noted that northeastern Bangladesh causes orographic uplifting and convective overturning of low-level moist air from the BoB, which might have implications in spatiotemporal precipitation changes.

The ocean-atmospheric circulation indexes like Nino3.4, SOI, SASMI, EASMI, and MJO are essential in determining monsoon precipitation distribution (Rahman and Islam, 2019). Wang et al. (2017) noted that the monsoon climate's inter-annual change might derive from thermodynamic

feedback systems, including Nino3.4 and SOI. Rahman and Islam (2019) identified SASMI and EASMI as an influencing factor of precipitation in Bangladesh, supporting our result as SASMI and EASMI have a significant relationship with monsoon precipitation in the form of moderate precipitation indices. Akhouri and Avishek (2019) identified a strong correlation between SOI and monsoon precipitation in India, not matching our results. On the contrary, Revadekar and Kulkarni (2008) identified strong correlations between the intensity and frequency of extreme precipitation events and Nino3.4 in India, which is similar to our result in the sense of light precipitation. Moron and Robertson (2014) also found a weak correlation between monsoon rainfall of West Bengal (adjacent to Bangladesh) and Nino3.4 and SST during June–September. Hossain et al. (2001) noticed a reduction of precipitation in the eastern region of Bangladesh owing to the adverse effects of SOI during El Niño episodes, which does not support our result as SOI did not exhibit a significant correlation with

the precipitation indices, although very heavy precipitation shows high coherency with SOI. The possible cause is that the wind flow is predominantly easterlies at the lower levels with strong westerlies above during the El Niño years. This scenario produces a vertical wind shear in the region, which suppressed the cyclone genesis; hence, strong easterly waves can be associated with heavy precipitation in Bangladesh. The MJO is also regarded as an influential factor for cyclogenesis on a global scale (Roman-Stork and Subrahmanyam 2020). Anandh and Vissa (2020) found that during the Indian summer monsoon, extreme rainfall events are strongly associated with the active and suppressed phase of MJO over the east coast of India, which contradicts our results. We found that MJO is associated with the light precipitation indices only.

Nonetheless, monsoon precipitation patterns in Bangladesh were changing in the contexts of decreasing light precipitation events and increasing heavy precipitation events. Besides, the indices were found responsive to ocean-atmospheric circulations. Therefore, protection of agriculture, ecosystem, fish culture, water resources, and thus, the country's overall economy from frequent flooding during the monsoon season is required. The findings of this study can be helpful in the aspect of better decision-making to adopt adequate flood prevention techniques and planning water resources use and management in Bangladesh. However, anthropogenic activities like natural resources exploitation, land use pattern change, burning fossil fuel and greenhouse gas emission, deforestation, evaporation paradox, and cloud microphysics for aerosol loading might influence the monsoon precipitation system in Bangladesh. Hence, future research should focus on the specific impacts of local drivers or other global climatic cycles. Also, owing to the interconnected nature of several large-scale oscillations, statistical approaches such as Pearson correlation analysis and wavelet analysis cannot clearly separate the interaction effect of numerous climatic oscillations. As a result, this study was conducted without explicitly analyzing the interrelationships between various climatic cycles.

5 Conclusion

This study developed and evaluated ten threshold-based precipitation indices for the monsoon season to investigate the spatiotemporal changes in monsoon precipitation patterns in Bangladesh for the 1980–2017 period. Wavelet transform coherence analysis was adopted to explore the teleconnection between the monsoon precipitation indices and the large-scale ocean-atmospheric circulation indices. Multiple wavelet coherence was employed to examine the relationship between these indices under the influences of the synoptic circulation

patterns. The probable mechanisms behind the changes in monsoon precipitation patterns in Bangladesh were also investigated. This study led to the following significant conclusions:

1. The light and moderate monsoon precipitation indices decreased, while the heavy precipitation indices increased significantly in Bangladesh during 1980–2017. On a spatial scale, most indices showed decreasing tendency predominantly in the northwest, while increasing tendency in the country's southeast.
2. The monsoon precipitation indices showed some remarkable teleconnection with the large-scale ocean-atmospheric indices. For example, light precipitation indices showed a significant negative correlation with Niño3.4 and MJO, while moderate precipitation amounts showed a significant positive association with SASMI and EASMI. Besides, the moderate precipitation day and very heavy precipitation amount showed significant association with SASMI and SOI, respectively. Wavelet coherence analysis also revealed strong coherence between these indices.
3. The ECMWF-ERA5 reanalysis data exhibited significant increases in SST, temperature, and geopotential height at 850 hPa, total precipitation rate, and summer evaporation, and decrease in MVIMD, which might influence the changing monsoon precipitation patterns over Bangladesh in recent years. Pearson correlation and multiple wavelet coherence analysis also affirmed the influence of these indices on the monsoon precipitation indices.
4. The outcomes of this study can provide an understanding of the impacts of monsoon climate variability on agriculture, especially for growing crops and harvesting. This output can also provide an understanding of potential drought and flood in monsoon in different regions of Bangladesh. The information generated in this study can be used to manage, monitor, and anticipate floods; predict future precipitation patterns; and enhance early warning systems. Besides, the methodology adopted in this study can be replicated in other regions, considering the climatic conditions are similar.
5. The limitation of this study lies in two perspectives. First, this study did not consider the station-wise teleconnection between the precipitation and ocean-atmospheric indices, rather considered the country average. Second, global climate change scenarios and other global climatic oscillation indices, i.e., Atlantic Multidecadal Oscillation, Pacific Decadal Oscillation, and North Atlantic Oscillation, were not considered in this study. However, future studies should focus on closing these shortcomings, along with analyzing the relationship between anthropogenic activities and monsoon precipitation system in Bangladesh.

Supplementary Information The online version contains supplementary material available at <https://doi.org/10.1007/s00704-022-03996-8>.

Acknowledgements The authors highly acknowledge the Bangladesh Meteorological Department (BMD) for providing the required datasets to conduct this study. The authors also acknowledge the NCEP/NCAR and ECMWF ERA5 reanalysis datasets used in this study. The authors also thank the Department of Disaster Management, Begum Rokeya University, Rangpur, for providing the necessary supports to conduct this study.

Author contribution Azad, M. A. K., designed, conceptualized, drafted the original manuscript; Islam, A. R. M. T.; Azad, M. A. K.; and Rahman, M. S. planned the documents; Azad, M. A. K., and Ayen, K., involved in the literature review, software, mapping, statistical analysis, interpretation of the analysis and discussion; Ayen, K., contributed to instrumental setup, data analysis, validation; Azad, M. A. K.; Ayen, K.; and Rahman, M. S., contributed to data collection and extraction; Islam, A. R. M. T.; Mallick, M.; and Shahid, S., had done the internal review and proofreading during the manuscript drafting stage.

Funding The authors extend their appreciation to the Deanship of Scientific Research at King Khalid University for funding this work through Research Group under grant number (RGP2/169/43).

Data availability Data will be available upon reasonable request on corresponding authors.

Code availability Code will be available upon reasonable request on corresponding authors.

Declarations

Ethical approval Not applicable.

Consent to participate Not applicable.

Consent for publication Not applicable.

Conflict of interest The authors declare no competing interests.

References

- Ahasan M, Chowdhary MA, Quadir D (2011) Variability and trends of summer monsoon rainfall over Bangladesh. *J Hydrol Meteorol* 7(1):1–17. <https://doi.org/10.3126/jhm.v7i1.5612>
- Ahmed ASMS, Munim AA, Begum QN, Choudhury AM (1996) El Niño Southern Oscillation and rainfall variation over Bangladesh. *Mausam* 47(2):157–162
- Ahmed MK, Alam MS, Yousuf AHM, Islam MM (2017) A long-term trend in precipitation of different spatial regions of Bangladesh and its teleconnections with El Nino/southern oscillation and Indian Ocean dipole. *Theor Appl Climatol* 129(1–2):473–486. <https://doi.org/10.1007/s00704-016-1765-2>
- Akhoury G, Avishek K (2019) Statistical analysis of Indian rainfall and its relationship with the Southern Oscillation Index. *Arab J Geo* 12:255. <https://doi.org/10.1007/s12517-019-4415-z>
- Anandh PC, Vissa NK (2020) On the linkage between extreme rainfall and the Madden–Julian Oscillation over the Indian region. *Meteorol Appl* 27:1901. <https://doi.org/10.1002/met.1901>
- Ashfaq M, Shi Y, Tung WW, Trapp RJ, Gao X, Pal JS, Diffenbaugh NS (2009) Suppression of south Asian summer monsoon precipitation in the 21st century. *Geophys Res Lett* 36:L01704. <https://doi.org/10.1029/2008GL036500>
- Azad MAK, Islam ARMT, Rahman MS, Ayen K (2021) Development of novel hybrid machine learning models for monthly thunderstorm frequency prediction over Bangladesh. *Natural Hazards* 108:1109–1135. <https://doi.org/10.1007/s11069-021-04722-9>
- Basher M, Stiller-Reeve MA, Saiful Islam AKM, Bremer S (2018) Assessing climatic trends of extreme rainfall indices over north-east Bangladesh. *Theor Appl Climatol* 134:441–452. <https://doi.org/10.1007/s00704-017-2285-4>
- Bhatt BC, Nakamura K (2005) Characteristics of monsoon rainfall around the Himalayas revealed by TRMM Precipitation Radar. *Mon Wea Rev* 133:149–165. <https://doi.org/10.1175/MWR-2846.1>
- BMD, 2018 Bangladesh Meteorological Department. Climate Data Portal. Government of Bangladesh, Agargaon, Dhaka. Available at: <http://bmd.wospace.org/team/homex.php>, Accessed date: 10 January 2019
- Chase TN, Knaff JA, Pielke RA, Kalnay E (2003) Changes in global monsoon circulations since 1950. *Nat Haz* 29:229–254. <https://doi.org/10.1023/A:1023638030885>
- Chaudhary S, Dhanya CT, Vinnarasi R (2018) Dry and wet spell variability during monsoon in gauge-based gridded daily precipitation datasets over India. *J Hydrol* 546:204–218. <https://doi.org/10.1016/j.jhydrol.2017.01.023>
- Chen X, Quan Q, Zhang K, Wei J (2021) Spatiotemporal characteristics and attribution of dry/wet conditions in the Weihe River Basin within a typical monsoon transition zone of East Asia over the recent 547 years. *Environ Model Softw* 143:105116. <https://doi.org/10.1016/j.envsoft.2021.105116>
- Donat MG, Lowry AL, Alexander LV, O’Gorman PA, Maher N (2016) More extreme precipitation in the world’s dry and wet regions. *Nat Clim Change* 6:508–513. <https://doi.org/10.1038/nclimate2941>
- Dubache G, Ogwang BA, Ongoma V, Islam ARMT (2019) The effect of Indian Ocean on Ethiopian seasonal rainfall. *Meteorol Atmos Phys* 131(6):1753–1761. <https://doi.org/10.1007/s00703-019-00667-8>
- Endo N, Matsumoto J, Hayashi T, Terao T, Murata F, Kiguchi M, Yamane Y, Alam MS (2015) Trends in precipitation characteristics in Bangladesh from 1950 to 2008. *SOLA* 11:113–117. <https://doi.org/10.2151/sola.2015-0272015>
- Fahad, A. A., Singh, B., Kamal, M., Ahmed, T., Kibria, M., & Chowdhury, N. R.,: 2021 The role of local topography and sea surface temperature on summer monsoon precipitation over Bangladesh and northeast India. *International Journal of Climatology* <https://doi.org/10.1002/joc.7490>
- Fujinami H, Sato T, Kanamori H, Murata F (2017) Contrasting features of monsoon precipitation around the Meghalaya Plateau under westerly and easterly regimes. *JGR Atmos* 122(18):9591–9610. <https://doi.org/10.1002/2016JD026116>
- Ghose B, Islam ARMT, Islam HMT, Hasanuzzaman M, Huang J, Hu Z, MoniruzzamanM, Gustave W, KarimM, Ibrahim, S.M.,: Rainfed rice yield fluctuation to climatic anomalies in Bangladesh. *Int J Plant Prod.* 15, 183–201. <https://doi.org/10.1007/s42106-021-00131-x>
- Grinsted A, Moore JC, Jevrejeva S (2004) Application of the cross wavelet transform and wavelet coherence to geophysical time series. *Nonlinear Process Geophys* 11:561–566. <https://doi.org/10.5194/npg-11-561-2004>
- Guilbert J, Betts AK, Rizzo DM, Beckage B, Bombles A (2015) Characterization of increased persistence and intensity of precipitation in the northeastern United States. *Geophys Res Lett* 42:1888–1893. <https://doi.org/10.1002/2015GL063124>

- Hassan, S.Q., Mallik, M.A.K., Akhter, M.A., Chowdhury, MAM.: 2015 Trend analysis and spatial distribution of monsoon precipitation over Bangladesh during 1951–2012, *Journal of Engineering Science*. 6(1–2), 75–80
- Hossain, E., Alam, S.S., Imam, K.H., Hoque, M.M.: 2001 Bangladesh country case study: impacts and response to the 1997–98 El Niño event. In: Glantz, M.H. (Ed.), *Once Burned Twice Shy? Vol - 1*. United Nations University Press, pp. 44–50. <https://doi.org/10.1007/s00703-019-00720-6>
- Huang Y, Wang H, Xiao W, Chen L, Yang H (2019) Spatiotemporal characteristics of precipitation concentration and the possible links of precipitation to monsoons in China from 1960 to 2015. *Theor Appl Climatol* 138:135–152. <https://doi.org/10.1007/s00704-019-02814-y>
- IPCC: 2013 *The Physical Science Basis. Contribution of Working Group I to the Fifth Assessment Report of the Intergovernmental Panel on Climate Change*. [Stocker, T.F., D. Qin, G.-K. Plattner, M. Tignor, S.K. Allen, J. Boschung, A. Nauels, Y. Xia, V. Bex and P.M. Midgley (eds.)]. Cambridge University Press, Cambridge, United Kingdom and New York, NY, USA. 1535 pp,
- Islam ARMT, Shen S, Yang S, Hu Z, Chu R (2019) Assessing recent impacts of climate change on design water requirement of Boro rice season in Bangladesh. *Theor Appl Climatol* 138(1–2):97–113. <https://doi.org/10.1007/s00704-019-02818-8>
- Islam ARMT, Islam HMT, Shahid S, Khatun MK, Ali MM, Rahman MS, Ibrahim SM, Almoajel AM (2021) Spatiotemporal nexus between vegetation change and extreme climatic indices and their possible causes of change. *J Environ Manag* 289:112505. <https://doi.org/10.1016/j.jenvman.2021.112505>
- Islam ARMT, Hasanuzzaman M, Azad MAK, Salam R, Toshi FZ, Khan MSI, Alam GMM, Ibrahim SM (2021) Effect of meteorological factors on COVID-19 cases in Bangladesh. *Environ Dev Sustain* 23:9139–9162. <https://doi.org/10.1007/s10668-020-01016-1>
- Islam, A.R.M.T., Rahman, M.S., Khatun, R., Hu, Z.: 2020 Spatiotemporal trends in the frequency of daily rainfall in Bangladesh during 1975–2017. *Theoret Appl Climatol* 141(3–4):869–887 <https://doi.org/10.1007/s00704-020-03244-x>
- Jerin JN, Islam HMT, Islam ARMT, Shahid S, Hu Z, Badhon MA, Chu R, Elbeltagi A (2021) Spatiotemporal trends in reference evapotranspiration and its driving factors in Bangladesh. *Theor Appl Climatol* 144:793–808. <https://doi.org/10.1007/s00704-021-03566-4>
- John R, Chen JQ, Lu N, Wilske B (2009) Land cover/land use change in semi-arid Inner Mongolia: 1992–2004. *Environ Res Lett* 4(4):45010–45019. <https://doi.org/10.1088/1748-9326/4/4/045010>
- Joshi MK, Rai A (2015) Combined interplay of the Atlantic multidecadal oscillation and the interdecadal Pacific oscillation on rainfall and its extremes over Indian subcontinent. *Clim Dyn* 44:3339–3359. <https://doi.org/10.1007/s00382-014-2333-z>
- Kendall, M.G.: 1975 Rank correlation measures. 1. Charles Griffin, London, pp. 25–55
- Khan, M.J.U., Islam, A.K.M.S., Das, M.K., Mohammed, K., Bala, S.K., Islam, G.M.T.: Observed trends in climate extremes over Bangladesh from 1981 to 2010. *Clim Res* 77:45–61 <https://doi.org/10.3354/cr01539>
- Khatun, M.A., Rashid, M.B., Hygen, H.O.: 2016 MET report on climate of Bangladesh. Section: Climate, Report no: 08/2016
- Lee E, Kim S (2019) Wavelet analysis of soil moisture measurements for hillslope hydrological Processes. *J Hydrol* 575:82–93. <https://doi.org/10.1016/j.jhydrol.2019.05.023>
- Li J, Zeng Q (2003) A new monsoon index and the geographical distribution of the global monsoons. *Adv Atmos Sci* 20:299–302. <https://doi.org/10.1007/s00376-003-0016-5>
- Li M, Chu R, Shen S, Islam ARMT (2018) Dynamic analysis of pan evaporation variations in the Huai River Basin, a climate transition zone in eastern China. *Sci Total Environ* 625:496–509. <https://doi.org/10.1016/j.scitotenv.2017.12.317>
- Lin L, Gettelman A, Xu Y, Wu C, Wang Z, Rosenbloom N, Bates SC, Dong W (2019) CAM6 simulation of mean and extreme precipitation over Asia: Sensitivity to upgraded physical parameterizations and higher horizontal resolution. *Geosci Model Dev* 12:3773–3793. <https://doi.org/10.5194/gmd-12-3773-2019>
- Liu WL, Zhang MJ, Wang SJ, Wang BL, Li F, Che Y (2013) Changes in precipitation extremes over Shaanxi Province, northwestern China, during 1960–2011. *Quat Int* 313–314:118–129. <https://doi.org/10.1016/j.quaint.2013.06.033>
- Loo YY, Billa L, Singh A (2015) Effect of climate change on seasonal monsoon in Asia and its impact on the variability of monsoon rainfall in Southeast Asia. *Geoscience Frontiers* 6:817–823. <https://doi.org/10.1016/j.gsf.2014.02.009>
- Luong MT, Castro CL, Chang H, Lahmers T, Adams DK, Ochoa-Moya CA (2017) The more extreme nature of North American monsoon precipitation in the Southwestern United States as revealed by a historical climatology of simulated severe weather events. *J Appl Met Clim* 56:2509–2529. <https://doi.org/10.1175/JAMC-D-16-0358.1>
- Lupikasza EB, Hänsel S, Matschullat J (2011) Regional and seasonal variability of extreme precipitation trends in southern Poland and central-eastern Germany 1951–2006. *Int J Climatol* 31:2249–2271. <https://doi.org/10.1002/joc.2229>
- Mann, H.B.: 1945 Non-parametric tests against trend. *Econometrica*. 13, 245–259 New York.
- Matsumoto, J.: 1988 Synoptic features of heavy monsoon rainfall in 1987 related to the severe floods in Bangladesh. *Bulletin of the Department of Geography, University of Tokyo*. 20, 43–56
- Meehl, G.A., Arblaster, J.M., Caron, J.M., Annamalai, H., Jochum, M., Chakraborty, A., Murtugudde, R.: 2012 Monsoon regimes and processes in CCSM4. Part I: the Asian-Australian monsoon. *Journal of Climate* 25 (8) 2583–2608 <https://doi.org/10.1175/JCLI-D-11-00184.1>
- Mie Sein ZM, Islam ARMT, Maw KW et al (2015) Characterization of southwest monsoon onset over Myanmar. *Meteorol Atmos Phys* 127(5):587–603. <https://doi.org/10.1007/s00703-015-0386-0>
- Montes C, Acharya N, Hassan SMQ, Krupnik TJ (2021) Intense precipitation events during the monsoon season in Bangladesh as captured by satellite-based products. *J Hydrometeorol* 22:1405–1419. <https://doi.org/10.1175/JHM-D-20-0287.1>
- Moron V, Robertson AW (2014) Interannual variability of Indian summer monsoon rainfall onset date at local scale. *Int J Climatol* 34:1050–1061. <https://doi.org/10.1002/joc.3745>
- Moron V, Robertson AW, Qian J (2010) Local versus regional-scale characteristics of monsoon onset and post-onset rainfall over Indonesia. *Clim Dyn* 34:281–299. <https://doi.org/10.1007/s00382-009-0547-2>
- Ng EKW, Chan JCL (2012) Geophysical applications of partial wavelet coherence and multiple wavelet coherence. *J Atmos Ocean Technol* 29(12):1845–1853. <https://doi.org/10.1175/JTECH-D-12-00056.1>
- Ozaki, M.: 2016 *Disaster Risk Financing in Bangladesh*. ADB South Asia Working Paper Series No. 46, September 2016. <https://doi.org/10.2139/ssrn.2941319>
- Pant GB (2003) Long-term climate variability and change over monsoon Asia. *J Indian Geophys Union* 7(3):125–134
- Ping Z, Xiuji Z, Longxun C, Jinhai HE (2009) Characteristics of subtropical monsoon and rainfall over Eastern China and Western North Pacific. *J Meteorol Res* 23(6):649–665
- Praveen B, Talukdar S, Shahfahad, Mahato S, Mondal J, Sharma P, Islam ARMT, Rahman A.: Analyzing trend and forecasting of rainfall changes in India using non-parametrical and machine learning approaches, *Scientific Report*, 10(1): 10342 <https://doi.org/10.1038/s41598-020-67228-7>

- Rafiuddin M, Uyeda H, Islam MN (2010) Characteristics of monsoon precipitation systems in and around Bangladesh. *Int J Climatol* 30:1042–1055. <https://doi.org/10.1002/joc.1949>
- Rahman MS, Islam ARMT (2019) Are precipitation concentration and intensity changing in Bangladesh overtimes? Analysis of the possible causes of changes in precipitation systems. *Sci Total Environ* 690:370–387. <https://doi.org/10.1016/j.scitotenv.2019.06.529>
- Rahman MR, Salehin M, Matsumoto J (1997) Trends of monsoon rainfall pattern in Bangladesh. *Bangladesh J Wat Resour* 14–18:121–138
- Rahman MA, Yunsheng L, Sultana N (2017) Analysis and prediction of rainfall trends over Bangladesh using Mann-Kendall, Spearman's rho tests and ARIMA model. *Meteorol Atmos Phys* 129:409–424. <https://doi.org/10.1007/s00703-016-0479-4>
- Rahman MS, Azad MAK, Hasanuzzaman M, Salam R, Islam ARMT, Rahman MM, Hoque MMM (2021) How air quality and COVID-19 transmission change under different lockdown scenarios? A case from Dhaka city. *Bangladesh Sci Total Environ* 762:143161. <https://doi.org/10.1016/j.scitotenv.2020.143161>
- Rana, M.M., Shafee, S., & Karmakar, S.,: 2007 Estimation of rainfall in Bangladesh by using Southern Oscillation Index. *Pakistan Journal of Meteorology*. 4(7)
- Revadekar JV, Kulkarni A (2008) The El Nino-Southern Oscillation and winter precipitation extremes over India. *Int J Climatol* 28:1445–1452. <https://doi.org/10.1002/joc.1639>
- Roman-Stork HL, Subrahmanyam B (2020) The impact of the Madden-Julian Oscillation on Cyclone Amphan (2020) and southwest monsoon onset. *Remote Sensing* 12:3011. <https://doi.org/10.3390/rs12183011>
- Roxy M (2014) Sensitivity of precipitation to sea surface temperature over the tropical summer monsoon region—and its quantification. *Clim Dyn* 43:1159–1169. <https://doi.org/10.1007/s00382-013-1881-y>
- Roxy MK, Ritika K, Terray P, Murtugudde R, Ashok K, Goswami BN (2015) Drying of the Indian subcontinent by rapid Indian Ocean warming and a weakening land-sea thermal gradient. *Nat Commun* 6:7423. <https://doi.org/10.1038/ncomms8423>
- Safdar F, Khokhar MF, Arshad M, Adil IH (2019) Climate change indicators and spatiotemporal shift in monsoon patterns in Pakistan. *Adv Meteorol* 2019:8281201. <https://doi.org/10.1155/2019/8281201>
- Salahuddin A, Isaac RH, Curtis S, Matsumoto J (2006) Teleconnections between the sea surface temperature in the Bay of Bengal and monsoon rainfall in Bangladesh. *Global Planet Change* 53(3):188–197. <https://doi.org/10.1016/j.gloplacha.2006.06.001>
- Sen PK (1968) Estimates of the regression coefficient based on Kendall's tau. *J Amer Stat Assoc* 63:1379–1389
- Serreze, M.C., Barry, R.G.,: 2010 Climate change. In: Barry, R.G., Chorley, R.J. (Eds.), *Atmosphere, Weather and Climate*. Routledge, Oxon,
- Shahid S (2010) Rainfall variability and the trends of wet and dry periods in Bangladesh. *Int J Climatol* 30(15):2299–2313. <https://doi.org/10.1002/joc.2053>
- Shahid S (2011) Trends in extreme rainfall events of Bangladesh. *Theor Appl Climatol* 104:489–499. <https://doi.org/10.1007/s00704-010-0363-y>
- Shukla RP, Tripathi KC, Pandey AC, Das IML (2011) Prediction of Indian summer monsoon rainfall using Niño indices: a neural network approach. *Atmos Res* 102(1–2):99–109. <https://doi.org/10.1016/j.atmosres.2011.06.013>
- Singh D, Tsiang M, Rajaratnam B, Diffenbaugh NS (2014) Observed changes in extreme wet and dry spells during the South Asian summer monsoon season. *Nat Clim Change* 4:456–461. <https://doi.org/10.1038/nclimate2208>
- Tong S, Li X, Zhang J, Bao Y, Bao Y, Na L, Si A (2019) Spatial and temporal variability in extreme temperature and precipitation events in Inner Mongolia (China) during 1960–2017. *Sci Total Environ* 649:75–89
- Turner AG, Annamalai H (2012) Climate change and the South Asian summer monsoon. *Nat Climate Change* 2:587–595. <https://doi.org/10.1038/nclimate1495>
- Wahiduzzaman, M., Luo, J.,: 2020 A statistical analysis on the contribution of El Niño- Southern Oscillation to the rainfall and temperature over Bangladesh. *Meteorol Atmos Phys* 1–14:55–68 <https://doi.org/10.1007/s00703-020-00733-6>
- Wang B, Liu J, Kim H, Webster PJ, Yim S (2012) Recent change of the global monsoon precipitation (1979–2008). *Climate Dynamics* 39:1123–1135. <https://doi.org/10.1007/s00382-011-1266-z>
- Wang X, Wang B, Xu X (2019) Effects of large-scale climate anomalies on trends in seasonal precipitation over the Loess Plateau of China from 1961 to 2016. *Ecol Indic* 107:105643. <https://doi.org/10.1016/j.ecolind.2019.105643>
- Wang, X., Hou, X., Wang, Y.,: Spatiotemporal variations and regional differences of extreme precipitation events in the Coastal area of China from 1961 to 2014. *Atmos. Res.* 197, 94–104 <https://doi.org/10.1016/j.atmosres.2017.06.022>
- Wu R (2017) Relationship between Indian and East Asian summer rainfall variations. *Adv Atmos Sci* 34:4–15. <https://doi.org/10.1007/s00376-016-6216-6>
- Wu Y, Wu S-Y, Wen J, Xu M, Tan J (2016) Changing characteristics of precipitation in China during 1960–2012. *Int J Climatol* 36:1387–1402. <https://doi.org/10.1002/joc.4432>
- Xu G, Osborn TJ, Matthews AJ, Joshi MM (2016) Different atmospheric moisture divergence responses to extreme and moderate El Niños. *Clim Dyn* 47:393–410. <https://doi.org/10.1007/s00382-015-2844-2>
- Xu Y, Li T, Shen S, Xu G, Islam ARMT et al (2020) Effects of cyclic variability in Pacific decadal oscillation on winter wheat production in China. *Int J Climatol* 41(4):2239–2252. <https://doi.org/10.1002/joc.6956>
- Yang, B., Zhang, Y., Qian, Y., Song, F., Leung, L.R., Wu, P., Guo, Z., Lu, Y., Huang, A.,: 2019 Better monsoon precipitation in coupled climate models due to bias compensation. *npj Clim Atmos Sci* 2 43 <https://doi.org/10.1038/s41612-019-0100-x>
- Yeşilirmak E, Atatanır L (2016) Spatiotemporal variability of precipitation concentration in western Turkey. *Nat Hazards* 81:1–18. <https://doi.org/10.1007/s11069-015-2102-2>
- Zeng Q, Zhang Y, Lei H, Xie Y, Gao T, Zhang L, Wang C, Huang Y (2019) Microphysical characteristics of precipitation during pre-monsoon, monsoon, and post-monsoon periods over the South China Sea. *Adv Atmos Sci* 36:1103–1120. <https://doi.org/10.1007/s00376-019-8225-8>
- Zhang KX, Pan SM, Cao LG, Wang Y, Zhao Y, Zhang W (2014) Spatial distribution and temporal trends in precipitation extremes over the Hengduan Mountains region, China, from 1961 to 2012. *Quat Int* 349:346–356. <https://doi.org/10.1016/j.quaint.2014.04.050>
- Zhang YT, Guan XD, Yu HP, Xie YK, Jin H (2017) Contributions of radiative factors to enhanced dryland warming over East Asia. *J Geophys Res Atmos* 122:7723–7736. <https://doi.org/10.1002/2017JD026506>
- Zhang, W., Zhou, T., Zou, L., Zhang, L., Chen, X., 2018 Reduced exposure to extreme precipitation from 0.5 °C less warming in global land monsoon regions. *Nat. Commun* 9 3153 <https://doi.org/10.1038/s41467-018-05633-3>

Publisher's note Springer Nature remains neutral with regard to jurisdictional claims in published maps and institutional affiliations.